BULLETIN OF THE POLISH ACADEMY OF SCIENCES
TECHNICAL SCIENCES
Vol. 53, No. 2, 2005

Investigation and modelling of rare-earth activated waveguide structures

W. WOLIŃSKI, M. MALINOWSKI*, A. MOSSAKOWSKA-WYSZYŃSKA, R. PIRAMIDOWICZ, and P. SZCZEPAŃSKI

Institute of Microelectronics and Optoelectronics, Warsaw University of Technology,
75 Koszykowa Str., 00-662 Warsaw, Poland

Abstract. In this paper the overview of the recent study on the rare-earth activated waveguides performed in the Optoelectronic Department of IMiO is presented. We reported on the development of rare earth-doped fluorozirconate (ZBLAN) glass fibers that allow a construction of a new family of visible and ultraviolet fiber lasers pumped by upconversion. Especially the performance of holmium devices is presented. The properties of laser planar waveguides obtained by the LPE process and the growth conditions of rare earths doped YAG layers are presented. In this paper we present also the theoretical study of the nonlinear operation of planar waveguide laser, as an example the microdisk Nd:YAG structure is discussed. We derived an approximate formula which relates the small signal gain in the Nd:YAG active medium and the laser characteristics, obtained for whispering-gallery modes and radial modes, to the output power and real parameters of the laser structure

Key words: waveguide lasers, laser materials, spectroscopy, upconversion, rare-earth ions.

1. Introduction

Diode-pumped, solid-state lasers have a wide variety of applications in the industrial, military, medical, and research sectors. Waveguide, active structures based on rare-earth doped fibers, planar structures or microdisk and spherical waveguides offer an attractive technology for micro-size lasers [1,2].

One of the recent important developments is the successful operation of fiber lasers, which offer the highest efficiencies and the best thermal working conditions among solid-state lasers. Active fibers not only could be easily coupled to optical telecommunication fiber components, but also give output powers exceeding kW cw range. Our work is oriented on the experimental investigation of active fibers based on Pr, Ho and Nd ZBLAN glass and on developing of the theoretical formulae for the threshold and the output intensities.

We develop a planar waveguide lasing geometry, which is well matched to that of a diode bar pumping reducing or eliminating the need for beam shaping. The experimental work is oriented on the technology and investigation of Nd, Yb and Pr activated YAG planar waveguides and general modelling of rare-earth -doped planar lasers is also presented.

Microdisk and spherical waveguides, resonators, and lasers are important optoelectronic devices because of the possibility of their implementation as compact and efficient passive or active devices, based on their high Q circular structure. Particularly microdisk lasers have low threshold when the low-order transverse-electric modes are dominant. Experimental results revealed a possibility of a narrow-band single-mode lasing and a high spontaneous emission coupling strength. Recently we performed a systematic study of the nonlinear operation of microdisk lasers. In particular, the laser characteristics obtained for whispering-gallery modes and radial modes revealed the behaviour of the optimal outcoupling coefficient as a function of the structure parameters.

2. Experimental

Experimental studies on optical waveguides were performed using various excitation sources and detectors and monochromators. CW UV excitation was obtained with a high power filtered xenon lamp, argon and krypton ion lasers and dye laser were also used as the excitation sources. Pulsed excitation was achieved with the optical parametric oscillator pumped by a frequency doubled or tripled Continuum Surelite II Nd:YAG laser (10 ns pulse length, 10 Hz repetition rate and 180 mJ energy per pulse at 532 nm). For pulsed excitation in the UV region the fourth harmonic of Nd:YAG laser was also used. The spectra were recorded using single and double grating monochromators with dispersion better than 8 Å/mm and detected by EMI 9789 or RCA C 31034-02 cooled AsGa photomultipliers, Ge or PbSe diodes. Data acquisition was obtained with a Stanford SR 4000 boxcar averager controlled with a PC computer. Fluorescence lifetime measurements were made using a Stanford SR430 multichannel analyzer. Most of experiments were performed at 300 K.

*e-mail: m.malinowski@elka.pw.edu.pl

3. Results

3.1. Short wavelength emission in Ho:ZBLAN fiber. In this part the problem of upconversion pumping of visible and UV emission in Ho^{3+} activated ZBLAN is presented. Trivalent rare-earth ion-doped ZBLAN fiber lasers are attractive devices for generating short wavelength radiation [3]. Due to the waveguiding effect and important interaction length multi-photon processes such as excited state absorption (ESA), energy transfer upconversion (ETU) and photon avalanche (PA) absorption, may produce population in the high lying states which energy exceeds that of the pump photon. Red, green and blue emissions have been reported in various RE^{3+} doped upconversion pumped ZBLAN systems but generation in the ultra-violet (UV) has only been observed in Nd^{3+} doped ZBLAN fiber pumped by 590 nm photons and operating in the ultraviolet at 381 nm [4].

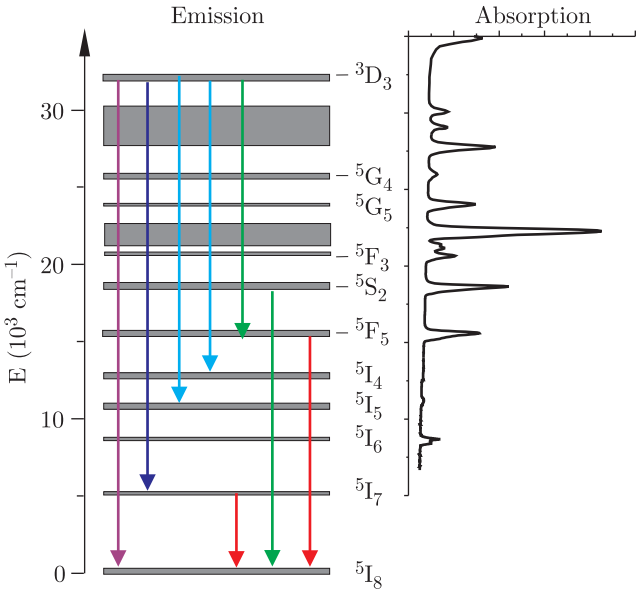

Fig. 1. Energy level scheme of Ho^{3+} ion in ZBLAN glass together with corresponding absorption spectrum

Holmium (Ho^{3+}) ion-doped upconversion fiber lasers are attractive devices for generating short wavelength radiation [5]. It was demonstrated that the green laser emission at 550 nm can be easily excited in Ho^{3+}:ZBLAN glass fiber after pumping with red diode laser [6,7]. Recently, we have reported on IR to visible up-conversion in holmium activated ZBLAN [8] and first observations of photon avalanche in holmium systems including Ho^{3+}:ZBLAN were reported in [9].

Here we report on the green (550 nm) blue (407 and 455 nm) and UV (309 and 355 nm) emissions in Ho^{3+}:ZBLAN fiber under upconversion pumping. Figure 1 shows the energy level scheme of Ho^{3+} ion in ZBLAN glass together with corresponding absorption spectrum. After cw UV (286.5 nm) excitation by a xenon lamp several emission lines were observed in a wide spectral range from UV to IR as seen in Fig. 1. Short wavelength fluorescence is dominated by two strong transitions, centered around 360 and 420 nm, originating from the $^3D_3$ to the $^5I_7$ and $^5I_6$ multiplets respectively. Emission centered on 480 nm is due to the $^5G_4 + {}^5F_3 \rightarrow {}^5I_8$ transitions when the main visible emission channel corresponding to the $^5S_2 \rightarrow {}^5I_8$ transition of Ho^{3+} ions is in the green part of the spectrum, at 550 nm.

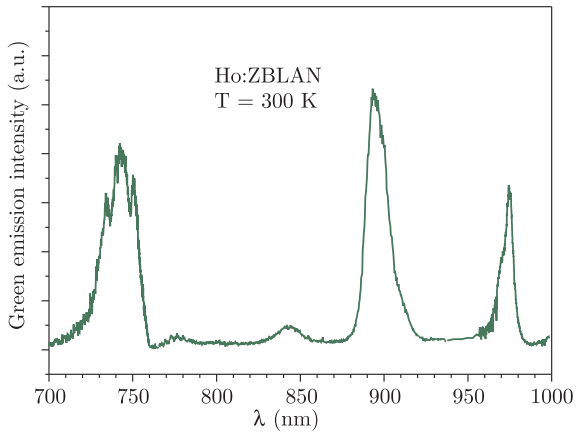

Fig. 2. Excitation spectrum of the green $^5S_2$ fluorescence of Ho^{3+} after excitation at several IR wavelength in the 720–770, 880–920 and 960–990 nm spectral ranges

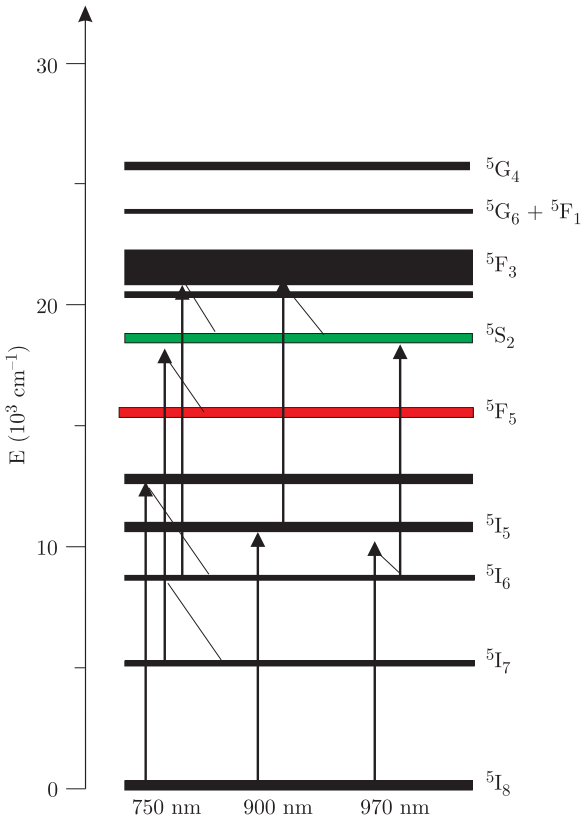

Fig. 3. Energy level diagram of Ho identifying excitation and emission wavelengths and showing possible GSA and ESA processes leading to population of the $^5F_5$, $^5S_2$ and $^5F_3$ states

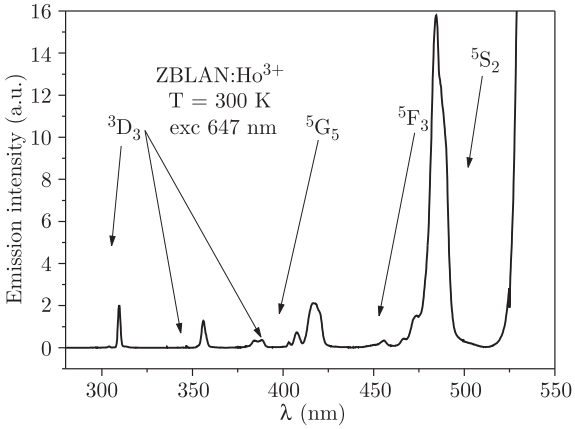

Fig. 4. Ultra violet and short wavelength part of visible spectrum after 647 nm pumping by krypton ion laser

Strong, green up-converted fluorescence of Ho^{3+} ion was observed after IR excitation in the 720–770, 880–920 and 960–990 nm spectral ranges, as shown in Fig. 2. In addition to the green signal corresponding to the $^5S_2 \rightarrow {}^5I_8$ transition, we also observed a weak emission in the blue region, at 490 nm, resulting from the $^5F_3 \rightarrow {}^5I_8$ transition. Figure 3 identifies the responsible ground state absorption (GSA), excited state absorption (ESA) and emission transitions.

Ultra violet emission from the $^3D_3$ state has been obtained using continuous, 647 nm pumping by krypton ion laser. Emission spectrum resulting from this excitation is shown in Fig. 4. It was observed that the intensity ration of the emission lines is dependent on excitation power. A nearly cubic $^3D_3$ intensity dependence on incident red pump power was determined, confirming the three-photon character of the observed process. The slopes of plots for 485 and 540 nm emission wavelengths are close to 2 indicating a two-photon excitation mechanism. From the energy level diagram of ZBLAN:Ho^{3+} presented in Fig. 1 it results that 647 nm excitation is resonant with the $^5F_5$ state. Under cw excitation the possible initial metastable states for the excited state absorption are $^5I_7$ and $^5I_6$. The $^5I_7$ state lifetime was determined to be 12.5 ms and $^5I_6$ has room temperature lifetime of 3.2 ms. The second, ESA absorption is to the $^5F_3$ or $^5G_5$ states, which relax nonradiatively to the green emitting $^5S_2$ metastable level. However, because of the low phonon character of the ZBLAN matrix, the $^5F_3$ or $^5G_5$ states decay also radiatively. The weak blue emission at 420 nm from the $^5G_5$ is observed in the emission spectrum in Fig. 4, which also confirms that the ESA from the $^5I_6$ is active indeed. The third step is also the ESA transition of the type $^5S_2 \rightarrow {}^3G_3 + {}^3L_8 + {}^3M_{10} + {}^5D_4$ terminating about 1900 cm^{-1} above the UV emitting $^3D_3$ state which is populated rapidly via non-radiative de-excitation. These upconversion excitation pathways are proposed in Fig. 5 together with the measured fluorescence lifetimes of the considered levels. For modelling the temporal behaviour of the UV emission after red pumping at 647 nm the rate equations were developed corresponding to the scheme shown in Fig. 5. The agreement between calculations and the experimental results confirms well the assumed excitation schemes.

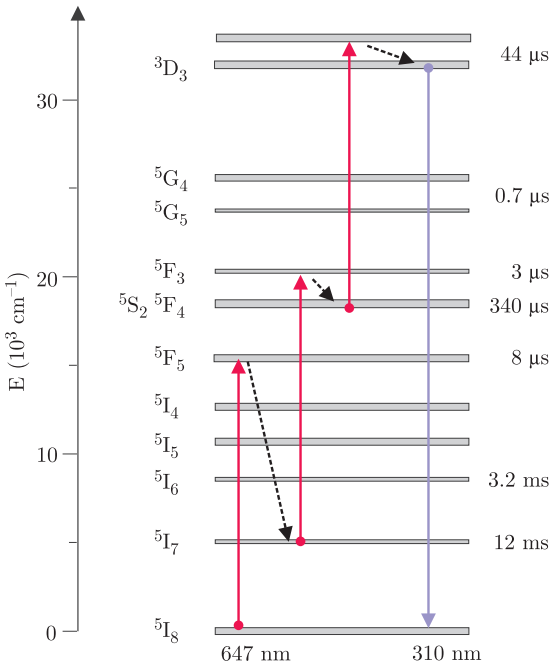

Fig. 5. Upconversion excitation pathways for the $^3D_3$ metastable state of holmium in ZBLAN

In conclusion, the visible and ultraviolet luminescence of Ho^{3+} ion in ZBLAN fiber has been studied under cw IR and red, 647 nm excitation. The dependence of the upconverted emission intensity versus pump power was measured. These results together with the measured fluorescence lifetime values allowed to propose the excitation scheme, which is successful absorption of two or three photons from the $^5I_7 + {}^5I_6$ and $^5S_2$ excited, intermediate states. In the next step the rate equation model was developed in order to study the dynamics of the proposed upconversion.

3.2. Planar waveguides. Planar active optical waveguides could be fabricated by a variety of techniques in numerous hosts including semiconductor materials, dielectric crystals and glasses. Depending on the type of substrate being used and the intended application such techniques as diffusion, liquid phase epitaxy (LPE), molecular beam epitaxy (MBE), implantation, physical vapour deposition and ionic exchange have been reported to generate optical waveguides.

Liquid phase epitaxy (LPE) is a promising technique for producing low loss (<0.05 dB/cm) planar waveguide lasers. In particular rare earth doped YAG epitaxial layers on YAG substrate have been demonstrated to have excellent laser properties [10,11]. Recently, in ITME laboratory in Warsaw thin LPE films of rare-earth activated YAG on YAG substrate have been obtained. Due to

gallium (Ga) substitution in the active layer the refractive index differences (n_f–n_c) up to 5×10^{-2} could be produced. The introduction of a large concentration of gallium requires a lattice mismatch compensation with lutetium (Lu) [12]. Our interest is focused on technology and studies of Pr^{3+}, Er^{3+}, Yb^{3+} and Nd^{3+} activated YAG and GGG waveguides.

In [13] the spectroscopic properties relevant to blue laser action have been determined for various Pr^{3+} activated materials. It was shown that on the basis of the simple spectroscopic measurements it is possible to develop a more complete picture of the potential performance of blue wavelength waveguide structures. The key results of the presented model were expressions for the threshold and gain dependencies on pump power and for dynamic parameters of the planar waveguide blue laser with Fabry-Perot as well as distributed feedback resonators. These equations include constants, such as the cross sections and lifetimes, easily obtained by simple spectroscopic measurements. From our analysis it resulted that the efficiency of the transverse pumped planar laser requires large absorption cross sections at pumping wavelength and has its optimum for a certain waveguide thickness, which generally is larger than required for fundamental mode operation. Among the studied hosts, the lowest threshold was predicted for Pr^{3+}:YAG/YAG waveguides. However, the calculated threshold pump power P_{th} value of about 200 W demonstrates practical difficulty in the transverse pumping of the waveguide lasers. It is anticipated that longitudinal pumping presents advantages in terms of lower laser excitation threshold, and will be considered in forthcoming paper.

In the Pr^{3+} doped GGG epitaxial planar film the IR to blue wavelength upconversion mechanism was investigated [14]. It was determined that the first photon is absorbed nonresonantly by a weak phonon band associated with the $^3H_4 \rightarrow {}^1G_4$ transition, the second resonant step is from the $^1G_4$ to the $^3P_0$ or one of the $^1I_6$ levels. Our low temperature excitation, emission and upconversion excitation spectra allowed us to determine the position of the Stark levels in the $^1G_4$ multiplet. These values extend the published data on the investigated system. For the first time emission spectrum in the 1.35 mm band originating from the $^1G_4$ state has been observed in Pr^{3+}:GGG system.

Recently Pr^{3+}:YAG thin films were used as substrates to manufacture the channel waveguides which are interesting as a possible laser structure operating in the green or blue region of visible spectrum [15]. The implantation technique was proposed for the preparation of such channel structures [16]. In crystalline materials, like e.g. Pr:YAG, ion implantation produces strongly damaged and strained area in the implanted region. It leads to the local changes in the refractive index, Fig. 6. Ion implanted optical channels are obtained by creating barriers of negative refractive index change in the implanted range compared with that in the layer [16,17]. Before implantation 12 μm wide and 4 μm thick gold mask was galvanicaly deposited on the surface of the wafer. The samples were implanted with H+ ions with energy of about 0.2 MeV and standard doses of $1 - 2 \times 10^{16}$ cm^{-2}.

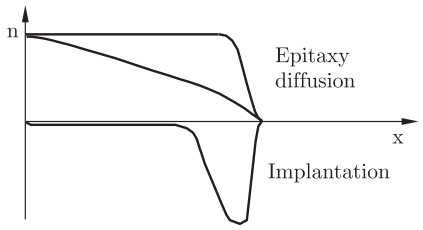

Fig. 6. Refractive index profiles for different planar waveguide technologies

Recently, much interest has been focused on Yb^{3+}-doped solid-state lasers. Efficient, diode-pumped room temperature, bulk Yb^{3+}:YAG laser were presented in 1991 by Lacovara et al. [18]. Recently, Pelenc et al. reported the 1.03 μm and 1.05 μm laser operation of a diode-pumped Yb^{3+} doped YAG planar waveguide [19]. Ytterbium activated YAG films were grown by means of LPE technique and the estimated optical losses at the laser wavelength were less than 0.1 dB/cm. The resonator consisted of two plane parallel mirrors with the 2.3% output transmission at 1.03 μm. An InGaAs 1W diode laser emitting around 968 nm was used as the pump. Energy level diagram for Yb^{3+} ion in YAG and the waveguide laser pump/output characteristic of the discussed device are presented in [20]. Very high slope efficiency, of about 77% and low thresholds of about 43 mW were registered, which are better than observed in bulk Yb^{3+}:YAG systems.

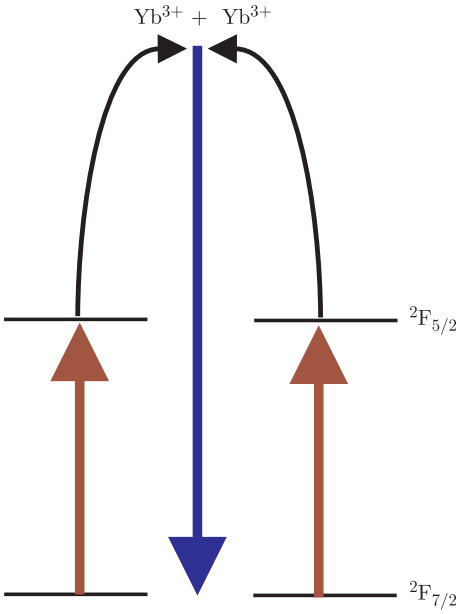

Fig. 7. Cooperative emission scheme of Yb^{3+} ions

In [21] we reported on the blue emission in Yb^{3+} activated YAG planar waveguides obtained by the liquid

phase epitaxy on YAG substrates and in bulk Yb^{3+}:YAG crystals under infrared excitation. Through the excitation and emission spectra, decay time measurements and excitation intensity dependence of the process responsible for this anti-Stokes emission was assigned to the cooperative deexcitation of two Yb^{3+} ions, see Fig. 7. Theoretical cooperative emission spectrum and the cooperative luminescence rate of Yb^{3+}:YAG waveguide were calculated, Fig. 8. It was shown that in the conditions of light guiding and high concentration of ytterbium this process is relatively efficient and observable even at low excitation powers.

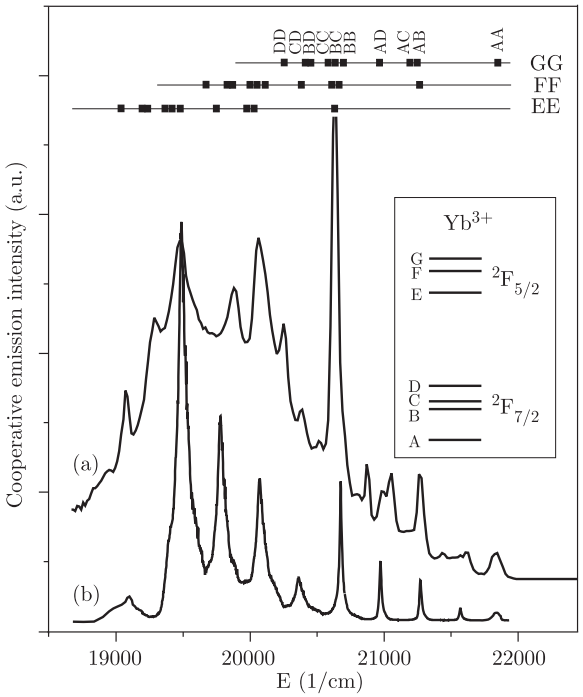

Fig. 8. Comparison of measured and calculated cooperative emission spectrum

3.3. Microdisk planar Nd:YAG laser. Microdisk lasers are important optoelectronic devices because of the possibility of their implementation as compact devices based on their high quality circular structure. They are characterized by low threshold and the domination of low-order transverse-electric (TE) mode. Experimental results also revealed a possibility of a narrow-band single-mode lasing and a high spontaneous emission coupling strength [22]. The design and optimization of microdisk lasers is critically dependent on the Q factor of the resonant optical modes, on the spectral and spatial overlap of these modes with the active medium and on the gain saturation effect. In most of the theoretical descriptions these lasers were studied considering whispering gallery modes [23–25].

In [26] we presented a systematic study of the nonlinear operation of microdisk Nd:YAG laser of geometry shown in Fig. 9. R1 is the radius of the disk and W is its thickness, the reflection coefficient ρ_{R1} characterizes the reflection from the outside surface of microdisk. In our approach we have started from vector-wave self-consisted mode equations taking into account three-dimensional spatial field dependence of laser modes. First we solved the threshold conditions, obtaining threshold gain and spectrum for radial modes. Next we included gain saturation effect. On the basis of the energy conservation theorem we derived an approximate formula which relates the small signal gain in the Nd:YAG active medium to the real parameters of the laser structure.

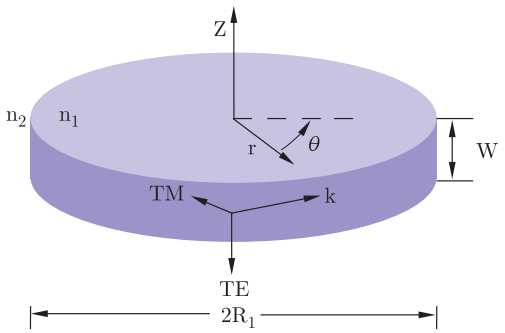

Fig. 9. Planar microdisk laser structure

The characteristics of the normalized small signal gain of Nd:YAG microdisk laser were calculated. The numerical results were obtained for laser operating at $\lambda = 1.064$ μm, the waveguide width W was 0.3 μm for fundamental mode TE00 and the radius of the structure was R1 = 50 μm.

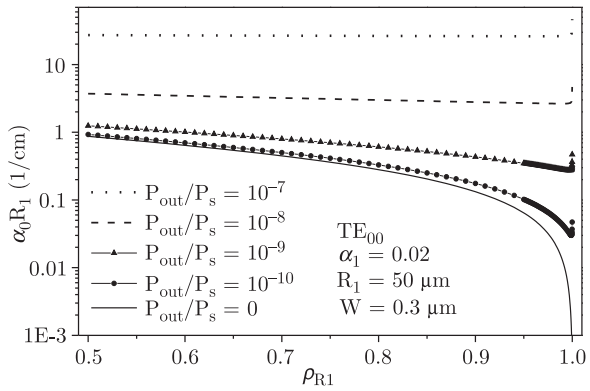

Fig. 10. Normalized small signal gain $\alpha_0 R_1$ versus the reflection coefficient ρ_{R1} with P_{out}/P_s as a parameter, of the TE_{00} mode, the losses in active region $\alpha_1 = 0.02$, microdisk radius $R_1 = 50$ μm and thickness W = 0.3 μm

In Fig. 10, the normalized small signal gain coefficient $\alpha_0 R_1$ is plotted against the reflection coefficient ρ_{R1} with the normalized output power P_{out}/P_s level as a parameter for Nd:YAG microdisk. It could be seen that the required small signal gain for given output power level decreases with increasing ρ_{R1} and the gain is less sensitive to ρ_{R1} for higher output power level. It is also important, that all curves go through a minimum within the range of presented values. Thus, for each power level, there exists an

optimum reflection strength that results in the minimum small signal gain required to maintain output power level. The minimum is broad for high output power values and becomes sharper for lower power levels.

4. Conclusions

We presented an overview of some of the recent results on active waveguide structures obtained in our laboratory. Three different topics were described, the problem of upconversion pumping of UV emission in holmium activated ZBLAN fiber, the spectroscopy of planar waveguides produced by liquid phase epitaxy and the theoretical description and modelling of planar lasers. For full details, references to relevant papers are given.

References

[1] R. Scheps, "Upconversion laser processes", *Prog. Quantum Electr.* 20, 271–358 (1996).

[2] R. Burkhalter, I. Dohnke, and J. Hullinger, "Growing of bulk crystals and structuring waveguides of fluoride materials for laser applications", *Progress in Crystals Growth and Characterization of Materials* 42, 1–64 (2001).

[3] D.S. Funk and J.G. Eden, "Glass fiber lasers in the ultraviolet and visible" *IEEE J. Select. Topics Quantum Electron.* 1, 784–791 (1995).

[4] D.S. Funk, J.G. Eden, J.S. Osinski, and B. Lu, "Green, holmium-doped upconversion laser pumped by red semiconductor laser", *Electron. Lett.* 33, 1958–1959 (1999).

[5] J.Y. Allain, M. Monerie, and H. Poignant, "Room temperature cw tunable green upconversion holmium fibre laser", *Electron. Lett.* 26, 261–262 (1990).

[6] David S. Funk. S.B. Stevens, S.S. Wu, and J. Gary Eden, "Tuning, temporal, and spectral characteristics of the green ($\lambda \sim 549$ nm), holium-doped fluorozirconate glass fiber laser", *IEEE JQE* 32, 638–645 (1996).

[7] D.S. Funk and J.G. Eden, "Laser diode pumped holmium doped fluorozirconate glass fiber laser in the green ($\lambda =$ 544–549 nm): power conversion, efficiency, pump acceptance bandwidth, and excited state kinetics", *IEEE JQE* 37, 980–992 (2001).

[8] A. Wnuk, M. Kaczkan, R. Piramidowicz, R. Mahiou, G. Bertrand, M.-F. Joubert, and M. Malinowski, "Dynamics of the up-conversion emission in holmium doped ZBLAN fiber", *Rad. Eff. Defects in Solids* 158, 469–473 (2003).

[9] M. Malinowski, A. Wnuk, Z. Frukacz, G. Chadeyron, R. Mahiou, S. Guy, and M.F. Joubert, "Room temperature photon avalanche in Ho^{3+} doped YAG, YAP, YLF and ZBLAN", *J. Alloys Comp.* 323–324, 731–735 (2001).

[10] P. Mockel, R. Plattner, W. Kruhler, A. Reichelt, and J. Grabmaier, "Miniature neodymium lasers (MNL) as possible transmitters for fiber-optic communication systems, Part 2. YAG:Nd^{3+} waveguide lasers", *Siemens Forsch.-u. Entwickl.-Ber. Bd.* 5, 296–302 (1976).

[11] N. Sugimoto, Y. Ohishi, Y. Katoh, A. Tate, M. Shimokozano, and S. Sudo, "A ytterbium- and neodymium-codoped yttrium aluminum garnet-buried channel waveguide laser pumped at 0.81 mm", *Appl. Phys. Lett.* 67, 582–584 (1995).

[12] M. Malinowski, J. Sarnecki, R. Piramidowicz, P. Szczepański, and W. Woliński, "Epitaxial RE^{3+}:YAG planar waveguide lasers", *Opto-Electron. Rev.* 9, 67–74 (2001).

[13] M. Malinowski, A. Mossakowska-Wyszyńska, R. Piramidowicz, P. Szczepański, A. Tyszka-Zawadzka, Z. Frukacz, and I. Pracka, "Modelling of blue wavelength praseodymium waveguide lasers", *Acta Physica Polonica* 97, 295–313 (2000).

[14] M. Malinowski, R. Piramidowicz, J. Sarnecki, and W. Woliński, "Infrared-to-blue wavelengths upconversion in GGG:Pr3+ thin film grown by liquid phase epitaxy", *J. Phys. Condens. Matter.* 10, 1–8 (1998).

[15] M. Nakielska, A. Wnuk, J. Sarnecki, and G. Gawlik, "Pr:YAG channel waveguides fabricated by H^+ ion implantation", *VIII Electron Technology Conference ELTE 2004, Stare Jabłonki*, FO-13, 320 (2004).

[16] P. Moretti, M.F. Joubert, S. Tascu, B. Jacquier, M. Kaczkan, M. Malinowski, and J. Sarnecki, "Luminescence of Nd^{3+} in proton or helium-implanted channel waveguides in Nd:YAG crystals" *Optical Materials* 24, 315–319 (2003).

[17] Y. Zhao, S.L. LaRochelle, E.J. Knystautas, N. Belanger, and A. Villeneuve, "Planar waveguides in ZBLAN fabricated by He ion implantation", *IPR paper* Ith17, 174–176 (2000).

[18] P. Lacovara, H.K. Choi, C.A. Wang, R.L. Aggarwal, and T.Y. Fan, "Room-temperature diode-pumped Yb:YAG laser", *Optics Letters* 16 (14), 1089–1091 (1991).

[19] D. Pelenc, B. Chambaz, I. Chartier, B. Ferrand, C. Wyon, D.P. Shepherd, D.C. Hanna, A.C. Large, and A.C. Tropper, "High slope efficiency and low threshold in a diode pumped epitaxially grown Yb:YAG waveguide laser", *Opt. Commun.* 115, 491–497 (1995).

[20] D. Pelenc, "Elaboration par epitaxie en phase liquide et caracterisation de couches monocristallines de YAG dope, realisation de laser guides d'onde neodyme et ytterbium a faibles seuils", *Ph. D. Thesis*, Universite J. Fourieur, Grenoble, 1993.

[21] M. Malinowski, M. Kaczkan, R. Piramidowicz, Z. Frukacz, and J. Sarnecki, "Cooperative emission in Yb^{3+}:YAG planar epitaxial waveguides", *Journal of Luminescence* 94–95, 29–33 (2001).

[22] L. Djaloshinski and M. Orenstein, "Disk and ring microcavity lasers and their concentric coupling", *IEEE J. Quantum Electron.* 35, 737–743 (1999).

[23] S.L. McCall, A.F.J. Levi, R. E. Slusher, S.J. Pearton, and R.A. Logan, "Whispering-gallery mode microdisk lasers", *Appl. Phys. Lett.* 60, 289–291 (1992).

[24] N.C. Frateschi and A.F.J. Levi, "Resonant modes and laser spectrum of microdisk lasers", *Appl. Phys. Lett.* 66, 2932–2934 (1995).

[25] M.K. Chin, D.Y. Chu, and S.T. Ho, "Approximate solution of the whispering gallery modes and estimation of spontaneous emission coupling factor for microdisk lasers", *Opt. Commun.* 109, 467–471 (1994)

[26] M. Nakielska, A. Mossakowska-Wyszyńska, M. Malinowski, and P. Szczepański, "Nd:YAG microdisk laser generating in the fundamental nmode", *Opt. Commun.* 235, 435–443 (2004).